

Limits on Flavor Changing Neutral Currents in D^0 Meson Decays

A. Freyberger,¹ D. Gibaut,¹ K. Kinoshita,¹ P. Pomianowski,¹ S. Schrenk,¹ D. Cinabro,² B. Barish,³ M. Chadha,³ S. Chan,³ G. Eigen,³ J. S. Miller,³ C. O'Grady,³ M. Schmidtler,³ J. Urheim,³ A. J. Weinstein,³ F. Würthwein,³ D. M. Asner,⁴ M. Athanas,⁴ D. W. Bliss,⁴ W. S. Brower,⁴ G. Masek,⁴ H. P. Paar,⁴ J. Gronberg,⁵ C. M. Korte,⁵ R. Kutschke,⁵ S. Menary,⁵ R. J. Morrison,⁵ S. Nakanishi,⁵ H. N. Nelson,⁵ T. K. Nelson,⁵ C. Qiao,⁵ J. D. Richman,⁵ D. Roberts,⁵ A. Ryd,⁵ H. Tajima,⁵ M. S. Witherell,⁵ R. Balest,⁶ K. Cho,⁶ W. T. Ford,⁶ M. Lohner,⁶ H. Park,⁶ P. Rankin,⁶ J. Roy,⁶ J. G. Smith,⁶ J. P. Alexander,⁷ C. Bebek,⁷ B. E. Berger,⁷ K. Berkelman,⁷ K. Bloom,⁷ D. G. Cassel,⁷ H. A. Cho,⁷ D. M. Coffman,⁷ D. S. Crowcroft,⁷ M. Dickson,⁷ P. S. Drell,⁷ D. J. Dumas,⁷ R. Ehrlich,⁷ R. Elia,⁷ P. Gaidarev,⁷ B. Gittelmann,⁷ S. W. Gray,⁷ D. L. Hartill,⁷ B. K. Heltsley,⁷ C. D. Jones,⁷ S. L. Jones,⁷ J. Kandaswamy,⁷ N. Katayama,⁷ P. C. Kim,⁷ D. L. Kreinick,⁷ T. Lee,⁷ Y. Liu,⁷ G. S. Ludwig,⁷ J. Masui,⁷ J. Mevissen,⁷ N. B. Mistry,⁷ C. R. Ng,⁷ E. Nordberg,⁷ J. R. Patterson,⁷ D. Peterson,⁷ D. Riley,⁷ A. Soffer,⁷ C. Ward,⁷ P. Avery,⁸ C. Prescott,⁸ S. Yang,⁸ J. Yelton,⁸ G. Brandenburg,⁹ R. A. Briere,⁹ T. Liu,⁹ M. Saulnier,⁹ R. Wilson,⁹ H. Yamamoto,⁹ T. E. Browder,¹⁰ F. Li,¹⁰ J. L. Rodriguez,¹⁰ T. Bergfeld,¹¹ B. I. Eisenstein,¹¹ J. Ernst,¹¹ G. E. Gladding,¹¹ G. D. Gollin,¹¹ M. Palmer,¹¹ M. Selen,¹¹ J. J. Thaler,¹¹ K. W. Edwards,¹² K. W. McLean,¹² M. Ogg,¹² A. Bellerive,¹³ D. I. Britton,¹³ R. Janicek,¹³ D. B. MacFarlane,¹³ P. M. Patel,¹³ B. Spaan,¹³ A. J. Sadoff,¹⁴ R. Ammar,¹⁵ P. Baringer,¹⁵ A. Bean,¹⁵ D. Besson,¹⁵ D. Coppage,¹⁵ N. Coptly,¹⁵ R. Davis,¹⁵ N. Hancock,¹⁵ S. Kotov,¹⁵ I. Kravchenko,¹⁵ N. Kwak,¹⁵ S. Anderson,¹⁶ Y. Kubota,¹⁶ M. Lattery,¹⁶ J. K. Nelson,¹⁶ S. Patton,¹⁶ R. Poling,¹⁶ T. Riehle,¹⁶ V. Savinov,¹⁶ M. S. Alam,¹⁷ I. J. Kim,¹⁷ Z. Ling,¹⁷ A. H. Mahmood,¹⁷ J. J. O'Neill,¹⁷ H. Severini,¹⁷ C. R. Sun,¹⁷ S. Timm,¹⁷ F. Wappler,¹⁷ J. E. Duboscq,¹⁸ R. Fulton,¹⁸ D. Fujino,¹⁸ K. K. Gan,¹⁸ K. Honscheid,¹⁸ H. Kagan,¹⁸ R. Kass,¹⁸ J. Lee,¹⁸ M. Sung,¹⁸ A. Undrus,^{18,*} C. White,¹⁸ R. Wanke,¹⁸ A. Wolf,¹⁸ M. M. Zoeller,¹⁸ X. Fu,¹⁹ B. Nemati,¹⁹ S. J. Richichi,¹⁹ W. R. Ross,¹⁹ P. Skubic,¹⁹ M. Wood,¹⁹ M. Bishai,²⁰ J. Fast,²⁰ E. Gerndt,²⁰ J. W. Hinson,²⁰ T. Miao,²⁰ D. H. Miller,²⁰ M. Modesitt,²⁰ E. I. Shibata,²⁰ I. P. J. Shipsey,²⁰ P. N. Wang,²⁰ M. Yurko,²⁰ L. Gibbons,²¹ S. D. Johnson,²¹ Y. Kwon,²¹ S. Roberts,²¹ E. H. Thorndike,²¹ C. P. Jessop,²² K. Lingel,²² H. Marsiske,²² M. L. Perl,²² S. F. Schaffner,²² R. Wang,²² T. E. Coan,²³ J. Dominick,²³ V. Fadeyev,²³ I. Korolkov,²³ M. Lambrecht,²³ S. Sanghera,²³ V. Shelkov,²³ R. Stroynowski,²³ I. Volobouev,²³ G. Wei,²³ M. Artuso,²⁴ A. Efimov,²⁴ M. Gao,²⁴ M. Goldberg,²⁴ R. Greene,²⁴ D. He,²⁴ N. Horwitz,²⁴ S. Kopp,²⁴ G. C. Moneti,²⁴ R. Mountain,²⁴ Y. Mukhin,²⁴ S. Playfer,²⁴ T. Skwarnicki,²⁴ S. Stone,²⁴ X. Xing,²⁴ J. Bartelt,²⁵ S. E. Csorna,²⁵ V. Jain,²⁵ S. Marka²⁵

(CLEO Collaboration)

¹Virginia Polytechnic Institute and State University, Blacksburg, Virginia 24061

²Wayne State University, Detroit, Michigan 48202

³California Institute of Technology, Pasadena, California 91125

⁴University of California, San Diego, La Jolla, California 92093

⁵University of California, Santa Barbara, California 93106

⁶University of Colorado, Boulder, Colorado 80309-0390

⁷Cornell University, Ithaca, New York 14853

⁸University of Florida, Gainesville, Florida 32611

⁹Harvard University, Cambridge, Massachusetts 02138

¹⁰University of Hawaii at Manoa, Honolulu, Hawaii 96822

¹¹University of Illinois, Champaign-Urbana, Illinois 61801

¹²Carleton University, Ottawa, Ontario, Canada K1S 5B6
and the Institute of Particle Physics, Montréal, Québec, Canada

¹³McGill University, Montréal, Québec, Canada H3A 2T8
and the Institute of Particle Physics, Montréal, Québec, Canada

¹⁴Ithaca College, Ithaca, New York 14850

¹⁵University of Kansas, Lawrence, Kansas 66045

¹⁶University of Minnesota, Minneapolis, Minnesota 55455

¹⁷State University of New York at Albany, Albany, New York 12222

¹⁸The Ohio State University, Columbus, Ohio 43210

¹⁹University of Oklahoma, Norman, Oklahoma 73019

²⁰Purdue University, West Lafayette, Indiana 47907

²¹University of Rochester, Rochester, New York 14627

²²Stanford Linear Accelerator Center, Stanford University, Stanford, California 94309

²³Southern Methodist University, Dallas, Texas 75275

²⁴Syracuse University, Syracuse, New York 13244²⁵Vanderbilt University, Nashville, Tennessee 37235

(Received 10 January 1996)

Using the CLEO II detector at the Cornell Electron Storage Ring, we have searched for flavor changing neutral currents and lepton family number violations in D^0 meson decays. The upper limits on the branching fractions for $D^0 \rightarrow \ell^+\ell^-$ and $D^0 \rightarrow X^0\ell^+\ell^-$ are in the range 10^{-5} to 10^{-4} , where X^0 can be a π^0 , K_s^0 , η , ρ^0 , ω , \bar{K}^{*0} , or ϕ meson, and the $\ell^+\ell^-$ pair can be e^+e^- , $\mu^+\mu^-$, or $e^\pm\mu^\mp$. Although these limits are above the theoretical predictions, most are new or an order of magnitude lower than previous limits. [S0031-9007(96)00011-7]

PACS numbers: 13.20.Fc, 11.30.Hv, 12.60.-i, 14.40.Lb

In the standard model (SM), flavor changing neutral currents (FCNC) are expected to be very rare in charm decays, and lepton family number violations (LFNV) are strictly forbidden. The FCNC decays, $D^0 \rightarrow \ell^+\ell^-$ and $D \rightarrow X\ell^+\ell^-$, can occur at the one loop level in the SM from penguin and box diagrams as shown in Fig. 1, but are highly suppressed by the Glashow-Iliopoulos-Maiani mechanism [1] and by the small quark masses in the loop. The theoretical estimates for the FCNC branching fractions [2] are of order 10^{-9} for $D \rightarrow X\ell^+\ell^-$ and 10^{-19} for $D^0 \rightarrow \ell^+\ell^-$, due to the additional helicity suppression.

In addition to these short distance loop diagrams there are contributions from long distance effects that can be several orders of magnitude larger [2]. There are two categories: (1) photon pole amplitudes and (2) vector meson dominance (VMD). Both involve nonperturbative QCD factors that are difficult to calculate.

The photon pole model [Fig. 2(a)] is essentially a W -exchange decay with a virtual photon radiating from one of the quark lines. The amplitude behaves differently depending on whether the final state meson is a vector (V) or pseudoscalar (P). The dilepton mass distribution for $D \rightarrow V\ell^+\ell^-$ modes peaks at zero (small q^2) since the photon prefers to be nearly real. Contrarily, the pole amplitude for $D \rightarrow P\ell^+\ell^-$ decays vanishes for small dilepton mass because $D \rightarrow P\gamma$ is forbidden by angular momentum conservation.

The VMD model [Fig. 2(b)] proceeds through the decay $D \rightarrow XV^0 \rightarrow X\ell^+\ell^-$, where V^0 is an intermediate ρ^0 , ω , or ϕ vector meson. The V^0 mixes with a virtual photon which then couples to $\ell^+\ell^-$. The dilepton mass spectrum will have poles at the ρ^0 , ω , and ϕ masses due to real V^0 mesons decaying into $\ell^+\ell^-$. There will also

be another pole at zero dilepton mass from the photon propagator if X is a vector meson.

Observation of FCNC decays at rates that exceed the long distance contributions opens a window into physics beyond the standard model; LFNV decays may suggest leptoquarks or heavy neutral leptons with non-negligible couplings to e and μ . Measuring the long distance contributions is also intrinsically important since our understanding at the charm sector can then be used to estimate the long distance effects for $b \rightarrow s\gamma$, which can be as large as 20% of the total decay rate [3]. Extracting $|V_{td}/V_{ts}|$ from the ratio $\mathcal{B}(B \rightarrow \rho\gamma)/\mathcal{B}(B \rightarrow K^*\gamma)$ is possible only if the short and long distance contributions can be separated.

The data were collected with the CLEO II detector at the Cornell e^+e^- Storage Ring (CESR), which operates on and just below the $\Upsilon(4S)$ resonance. The CLEO II detector [4] is a large solenoidal detector with 67 tracking layers and a CsI electromagnetic calorimeter that provides efficient π^0 reconstruction. We have used an integrated luminosity of 3.85 fb^{-1} , which corresponds to $\sim 5 \times 10^6 e^+e^- \rightarrow c\bar{c}$ events.

We have searched for the FCNC and LFNV decays $D^0 \rightarrow \ell^+\ell^-$ and $D^0 \rightarrow X\ell^+\ell^-$, where X can be a π^0 , K_s^0 , η , ρ^0 , ω , \bar{K}^{*0} , or ϕ meson [5]. The $\ell^+\ell^-$ pair can be either e^+e^- or $\mu^+\mu^-$ for the FCNC decays, and $e^\pm\mu^\mp$ for the LFNV decays.

Charged tracks, except for pions from K_s^0 decays, are required to be consistent with coming from the primary interaction point. Charged pion and kaon candidates are required to have dE/dx and, when available, time-of-flight information consistent with that of true pions and kaons.

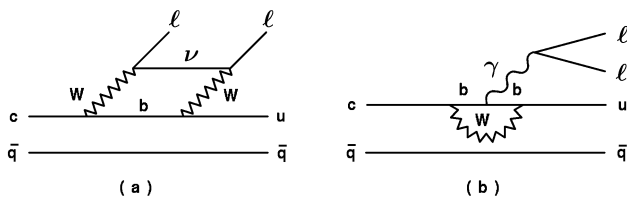


FIG. 1. Short distance contributions to FCNC decays in D mesons due to (a) box and (b) penguin diagrams.

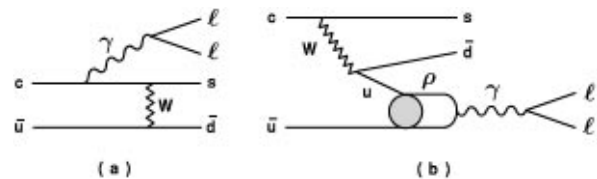


FIG. 2. Long distance contributions to FCNC decays in D mesons due to (a) photon pole amplitude and (b) vector meson dominance.

Electrons are identified by requiring that the energy deposition in the CsI calorimeter be consistent with the track momentum and the specific ionization loss (dE/dx) be consistent with that of true electrons. The electron candidate must have a momentum greater than $0.4 \text{ GeV}/c$ and satisfy $|\cos\theta| < 0.81$, where θ is the polar angle with respect to the beam axis. Electrons from photon conversions and π^0 Dalitz decays are rejected.

Muon candidates are selected by requiring the charged track to penetrate at least three nuclear interaction lengths of steel, which implicitly places a minimum momentum cut of $0.9 \text{ GeV}/c$. To further reduce the fake rate from pions we also require that the track lie in the region $|\cos\theta| < 0.7$ and that the CsI shower energy for the muon be less than 0.5 GeV .

The K_s^0 candidates are selected through the decay mode $K_s^0 \rightarrow \pi^+\pi^-$ by requiring a decay vertex displaced from the primary interaction point. The invariant mass of the K_s^0 candidates must be within $10 \text{ MeV}/c^2$ of its nominal value. The vector meson candidates are reconstructed through the decays $\rho^0 \rightarrow \pi^+\pi^-$, $\omega \rightarrow \pi^+\pi^-\pi^0$, $\bar{K}^{*0} \rightarrow K^-\pi^+$, and $\phi \rightarrow K^+K^-$. We require the candidates to have an invariant mass within 150, 20, 50, and $8 \text{ MeV}/c^2$ of their nominal mass, respectively.

We reconstruct the $\pi^0 \rightarrow \gamma\gamma$ decay mode from pairs of well-defined showers in the CsI calorimeter. The showers must not be matched to charged tracks and must have a lateral shower shape consistent with that of true photons. At least one photon must lie in the barrel region defined by $|\cos\theta| < 0.7$. The π^0 from the decay chain $D^0 \rightarrow \omega\ell^+\ell^-$, $\omega \rightarrow \pi^+\pi^-\pi^0$ ($D^0 \rightarrow \pi^0\ell^+\ell^-$) must have a momentum greater than 0.1 (0.6) GeV/c , and individual photon energies must be at least 0.03 (0.10) GeV , respectively. The π^0 from the $D^0 \rightarrow \pi^0\ell^+\ell^-$ mode has more stringent cuts since its momentum spectrum is harder. We select π^0 candidates that have an invariant mass within 2.5 standard deviations (σ) of the nominal mass. The photon four-momenta are kinematically fit to the nominal π^0 mass to improve the momentum estimate.

The decay $\eta \rightarrow \gamma\gamma$ is reconstructed in a similar procedure. In addition, η candidates are rejected if either photon is consistent with coming from a π^0 . The η momentum must be greater than $0.5 \text{ GeV}/c$ and each photon must have an energy of at least 0.15 GeV . We select η candidates that have an invariant mass within $30 \text{ MeV}/c^2$ of the nominal mass.

In order to reduce the combinatoric background, we require the D^0 candidates to come from $D^{*+} \rightarrow D^0\pi^+$ decays. Although $\sim 75\%$ of the D^0 sample is lost by imposing the D^{*+} tag, backgrounds are reduced by a factor of 20–40. We require the mass difference $M(D^{*+}) - M(D^0)$ to be within $2.0 \text{ MeV}/c^2$ (2σ) of its expected value. (The D^* tag is not required for the $D^0 \rightarrow \phi\ell^+\ell^-$ modes since their backgrounds are negligible.) Since charmed mesons from $e^+e^- \rightarrow c\bar{c}$ events are produced with a hard momentum spectrum, we further

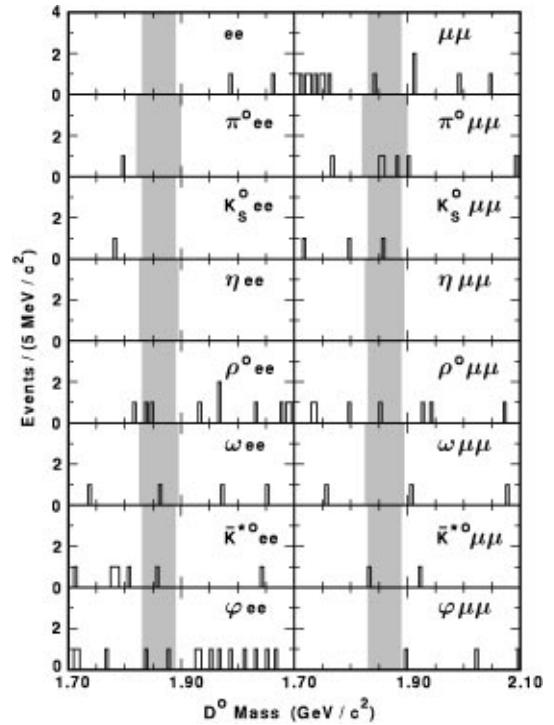


FIG. 3. Invariant mass distribution for FCNC D^0 decays. The signal region for the D^0 decay modes is shaded.

reduce the combinatoric background by requiring $x_p > 0.5$, where $x_p \equiv P_{D^{*+}}/\sqrt{E_{\text{beam}}^2 - M_{D^{*+}}^2}$ is the scaled momentum of the D^{*+} . Finally, the daughter particles of the D^0 candidate are required to lie within 90° of the D^0 momentum vector, which further reduces backgrounds in the $D^0 \rightarrow \rho^0\ell^+\ell^-$ and $\omega\ell^+\ell^-$ modes.

The invariant mass spectra for the FCNC and LFNV decays $D^0 \rightarrow \ell^+\ell^-$ and $D^0 \rightarrow X\ell^+\ell^-$ are shown in Figs. 3 and 4. We do not observe signals in any of the decay modes. The background levels are consistent with expectations from Monte Carlo (MC) simulations. The background combinatorics in the continuum MC are

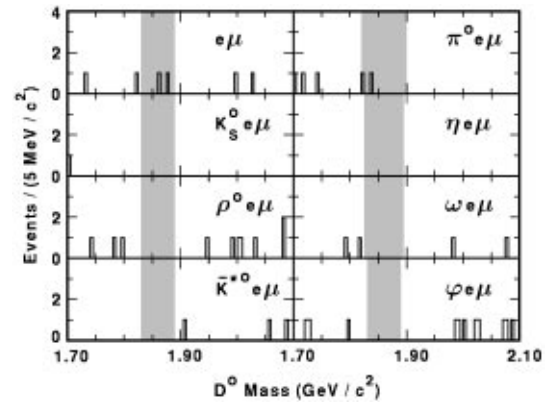


FIG. 4. Invariant mass distribution for LFNV D^0 decays. The signal region for the D^0 decay modes is shaded.

predominately from lepton fakes, whereas those in the BB MC are mainly from real leptons. We set upper limits on each mode by assuming all the events within 3σ of the D^0 mass (~ 30 MeV/ c^2) to be signal events. Assuming that the LFNV decay rates $D^0 \rightarrow Xe^+\mu^-$ and $D^0 \rightarrow Xe^-\mu^+$ are identical, we combine these two mass spectra together to obtain a more stringent limit on $D^0 \rightarrow Xe^\pm\mu^\mp$. The number of events in each signal region is shown in Table I.

The upper limit on branching fractions for the FCNC and LFNV decay modes is given by $\mathcal{B} = \lambda_n/\epsilon N_{D^0}$, where λ_n is the Poisson 90% upper limit for n observed events, ϵ is the reconstruction efficiency, and N_{D^0} is the number of D^0 mesons in the data, which is obtained from the observed $D^0 \rightarrow K^-\pi^+$ yield. We observe $70\,770 \pm 470$ events in the decay mode $D^0 \rightarrow K^-\pi^+$

TABLE I. Summary of upper limits on the FCNC and LFNV decay modes $D^0 \rightarrow \ell^+\ell^-$ and $D^0 \rightarrow X\ell^+\ell^-$. The efficiencies (\mathcal{E}) are for the phase space model and do not include branching fractions to the observed final states. The 90% C.L. upper limits are listed separately for the phase space (nonresonant) and photon pole amplitude decay models, together with previous limits.

Decay mode	Signal events	\mathcal{E} (%)	$\mathcal{B}(10^{-5})$ Upper limits		
			Nonres.	Pole	Previous
e^+e^-	0	14	1.3	...	13 [6]
$\mu^+\mu^-$	1	9	3.4	...	0.3 [7]
$e^\pm\mu^\mp$	2	11	19	...	10 [8]
$\pi^0 e^+e^-$	0	4.2	4.5	...	
$\pi^0 \mu^+\mu^-$	3	1.0	54	...	18 [9]
$\pi^0 e^\pm\mu^\mp$	2	2.5	8.6	...	
$\bar{K}^0 e^+e^-$	0	4.7	11	...	170 [10]
$\bar{K}^0 \mu^+\mu^-$	1	1.4	67	...	26 [9]
$\bar{K}^0 e^\pm\mu^\mp$	0	2.7	10	...	
ηe^+e^-	0	4.2	11	...	
$\eta \mu^+\mu^-$	0	0.9	53	...	
$\eta e^\pm\mu^\mp$	0	2.3	10	...	
$\rho^0 e^+e^-$	2	4.2	10	18	45 [11]
$\rho^0 \mu^+\mu^-$	1	0.7	49	45	25 [9]
$\rho^0 e^\pm\mu^\mp$	0	1.9	4.9	5.0	
ωe^+e^-	1	1.9	18	27	
$\omega \mu^+\mu^-$	0	0.3	83	65	
$\omega e^\pm\mu^\mp$	0	0.9	12	12	
$\bar{K}^{*0} e^+e^-$	1	3.4	14	20	
$\bar{K}^{*0} \mu^+\mu^-$	1	0.4	118	100	
$\bar{K}^{*0} e^\pm\mu^\mp$	0	1.4	10	10	
ϕe^+e^-	2	4.4	5.2	7.6	
$\phi \mu^+\mu^-$	0	0.2	41	24	
$\phi e^\pm\mu^\mp$	0	1.5	3.4	3.3	

for $x_p > 0.5$, and $17\,300 \pm 150$ events in the decay chain $D^{*+} \rightarrow D^0\pi^+$ with $D^0 \rightarrow K^-\pi^+$. This corresponds to 5.22×10^6 D^0 mesons and 1.38×10^6 $D^{*+} \rightarrow D^0\pi^+$ decays.

For the FCNC and LFNV modes we compute the D^0 reconstruction efficiency using a phase space decay of $D^0 \rightarrow X\ell^+\ell^-$. The efficiencies for $D^0 \rightarrow Xe^+e^-$ are about 4–10 times greater than those for $D^0 \rightarrow X\mu^+\mu^-$, due to the greater momentum acceptance for electrons. The efficiencies for the $D^0 \rightarrow V\ell^+\ell^-$ vector decay modes are also determined using a photon pole amplitude decay in which $D^0 \rightarrow V\gamma^* \rightarrow V\ell^+\ell^-$. This leads to a dilepton mass distribution of $d\Gamma/dm_{\ell\ell}^2 \propto 1/m_{\ell\ell}^2$. The $D^0 \rightarrow Ve^+e^-$ efficiency for the pole model is about 30% less than that of the phase space model, primarily due to low mass e^+e^- pairs that resemble photon conversions. We present upper limits in Table I using both decay model assumptions.

The main sources of systematic error are due to uncertainties in the efficiencies for charged particle tracking (2% per track), π^0 and η reconstruction (5%), lepton identification (6%), K_s^0 reconstruction (5%), and Monte Carlo statistics (4–8%). The total systematic errors are in the range (9–12)%, depending on the mode. We incorporate these errors into the upper limits by decreasing the efficiency by 1σ .

The upper limits on the branching fractions for the flavor changing neutral current and lepton family number violating decay modes are summarized in Table I. The 90% confidence level limits range from a few $\times 10^{-5}$ for $D^0 \rightarrow \ell^+\ell^-$, $\pi^0\ell^+\ell^-$, and $\phi\ell^+\ell^-$, to a few $\times 10^{-4}$ for the other decay modes. Although these limits are well above the theoretical predictions [2], the limits for $D^0 \rightarrow e^+e^-$, $e^\pm\mu^\mp$, and $K^0e^+e^-$ are an order of magnitude more restrictive than previous limits [6–11]. In addition, the limits for many other decay modes reported here are the first published constraints.

We gratefully acknowledge the effort of the CESR staff in providing us with excellent luminosity and running conditions. This work was supported by the National Science Foundation, the U.S. Department of Energy, the Heisenberg Foundation, the Alexander von Humboldt Stiftung, the Natural Sciences and Engineering Research Council of Canada, and the A. P. Sloan Foundation. One of us (D.F.) would like to thank Gustavo Burdman and Sandip Pakvasa for stimulating discussions.

*Permanent address: BINP, RU-630090 Novosibirsk, Russia.

- [1] S. L. Glashow, J. Iliopoulos, and L. Maiani, Phys. Rev. D **2**, 1285 (1970).
 [2] J. L. Hewett, Report No. SLAC-PUB-95-6821; S. Pakvasa, Report No. UH-511-787-94; A. J. Schwartz, Mod. Phys. Lett. A **8**, 967 (1993).

- [3] E. Golowich and S. Pakvasa, *Phys. Rev. D* **51**, 1215 (1995); J. Soares, Report No. TRI-PP-95-6; A. Khodjamirian *et al.*, *Phys. Lett. B* **358**, 129 (1995).
- [4] CLEO Collaboration, Y. Kubota *et al.*, *Nucl. Instrum. Methods Phys. Res., Sect. A* **320**, 66 (1992).
- [5] In this Letter the charge conjugate states are implied.
- [6] Mark III Collaboration, J. Adler *et al.*, *Phys. Rev. D* **37**, 2023 (1988).
- [7] E771 Collaboration, T. Alexopoulos *et al.*, Report No. FERMILAB-PUB-95-297-E; WA92 Collaboration, M. Adamovich *et al.*, *Phys. Lett. B* **353**, 563 (1995); E615 Collaboration, W. C. Louis *et al.*, *Phys. Rev. Lett.* **56**, 1027 (1986).
- [8] ARGUS Collaboration, H. Albrecht *et al.*, *Phys. Lett. B* **209**, 380 (1988).
- [9] E653 Collaboration, K. Kodama *et al.*, *Phys. Lett. B* **345**, 85 (1995).
- [10] Mark III Collaboration, J. Adler *et al.*, *Phys. Rev. D* **40**, 906 (1989).
- [11] CLEO Collaboration, P. Haas *et al.*, *Phys. Rev. Lett.* **60**, 1614 (1988).